

20 2017

ISSN 1301-2746

# ADALYA

The Annual of the Koç University Suna & İnan Kırac Research Center  
for Mediterranean Civilizations

(OFFPRINT)



**AKMED**

KOÇ UNIVERSITY

Suna & İnan Kırac

Research Center for

Mediterranean Civilizations

# ADALYA

The Annual of the Koç University Suna & İnan Kırac Research Center  
for Mediterranean Civilizations (AKMED)

<i>Mode of publication</i>	Worldwide periodical
<i>Publisher certificate number</i>	25840
ISSN	1301-2746
<i>Publisher management</i>	Koç University Rumelifeneri Yolu, 34450 Sariyer / İstanbul
<i>Publisher</i>	President Umran Savaş İnan on behalf of Koç University
<i>Editor-in-chief</i>	Oğuz Tekin
<i>Editor</i>	Tarkan Kahya
<i>Advisory Board</i>	Haluk Abbasoğlu, Jürgen Borchhardt, Thomas Corsten, Jacques des Courtils, Vedat Çelgin, Nevzat Çevik, İnci Delemen, Refik Duru, Serra Durugönül, Hansgerd Hellenkemper, Frank Kolb, Wolfram Martini, Mehmet Özdoğan, Mehmet Özsait, Urs Peschlow, Felix Pirson, Scott Redford, Denis Rousset, Christof Schuler, R. R. R. Smith, Oğuz Tekin, Gülsün Umurtak, Burhan Varkıvanç, Michael Wörrle, Martin Zimmerman
<i>English copyediting</i>	Mark Wilson
©	Koç University AKMED, 2017
	<b>Adalya, a peer reviewed publication, is indexed in the A&amp;HCI (Arts &amp; Humanities Citation Index) and CC/A&amp;H (Current Contents / Arts &amp; Humanities).</b>
<i>Production</i>	Zero Production Ltd. Abdullah Sok. No. 17 Taksim 34433 İstanbul Tel: +90 (212) 244 75 21 • Fax: +90 (212) 244 32 09 info@zerobooksonline.com ; www.zerobooksonline.com
<i>Printing</i>	Oksijen Basım ve Matbaacılık San. Tic. Ltd. Şti. 100. Yıl Mah. Matbaacılar Sit. 2. Cad. No: 202/A Bağcılar - İstanbul Tel: +90 (212) 325 71 25 • Fax: +90 (212) 325 61 99 Certificate number: 29487
<i>Mailing address</i>	Barbaros Mah. Kocatepe Sok. No. 25 Kaleiçi 07100 Antalya - TURKEY Tel: +90 (242) 243 42 74 • Fax: +90 (242) 243 80 13 <a href="https://akmed.ku.edu.tr">https://akmed.ku.edu.tr</a>
<i>E-mail address</i>	akmed@ku.edu.tr



KOÇ ÜNİVERSİTESİ



AKMED

KOÇ UNIVERSITY

Suna & İnan Kırac

Research Center for

Mediterranean Civilizations

# Contents

Rana Özbal <i>Reconsidering Identity in the Halaf World: A Study of Coarse Wares in Sixth Millennium North Mesopotamia</i> .....	1
Abdullah Hacı <i>İlk Tunç Çağı'na Tarihlenen Anadolu Metalik Çanak Çömleğine İlişkin Yeni Bilgiler: Göltepe Buluntuları</i> .....	21
Bekir Özer <i>Pedasa Athena Kutsal Alanı Arkaik Dönem Kıbrıs Mortarları ve Bölgeler Arası Ticari İlişkilerdeki Rolü</i> .....	41
Elçin Doğan Gürbüz – Cennet Pişkin Ayvazoğlu <i>Klaros'tan Pişmiş Toprak Barbitoslu Figürinlerin İkonografisi</i> .....	69
Gökhan Çoşkun <i>A One-Edged Curved Sword from Seyitömer Höyük</i> .....	83
Sevgi Sarıkaya <i>The Diplomatic and Strategic Maneuvers of Tissaphernes, Satrap of Sardis</i> .....	111
Marko Kiessel <i>Hof- und Fassadengräber auf der Karpashalbinsel Zyperns? Bemerkungen zu Kammergräbern in der Flur „Spiliosus“ nahe Aphendrika</i> .....	135
Erkan Dünder – Ali Akın Akyol <i>Unguentarium Production at Patara and a New Unguentarium Form: Archaeological and Archaeometric Interpretation</i> .....	157
Hülya Kökmen Seyirci <i>Ksanthos Güney Kent Kapısı ve Evreleri</i> .....	181
Julian Bennett <i>“Becoming a Roman”: Anatolians in the Imperial Roman Navy</i> .....	213
Lisa Peloschek – Martin Seyer – Banu Yener-Marksteiner – Philip Bes <i>Limestone, Diorite and Radiolarite: First Petrographic Data of Fired Clay Objects from Limyra (Southwest Turkey)</i> .....	241
Burhan Varkıvanç <i>The Stone Architecture of the Proskene of the Theater in Kaunos</i> .....	267
Ümit Aydınoglu <i>Doğu Dağlık Kilikia'daki Kırsal Yerleşimlerde Peristyl Avlulu Konutlar</i> .....	291

Pınar Özlem-Aytaçlar <i>Some Inscriptions from Pisidia</i> .....	315
Guntram Koch <i>Überlegungen zum Ende der Sarkophag-Produktion in Kleinasien</i> .....	323
Gökçen Kurtuluş Öztaşkın – Sinan Sertel <i>Olympos Piskoposluk Kilisesi'ndeki Nef Ayırımı Düzenlemeleri ve Levha Yanı Uygulaması</i> .....	357
Peter Talloen – Ralf Vandam – Manuela Broisch – Jeroen Poblome <i>A Byzantine Church Discovered in the Village of Ağlasun (Burdur): Some More Light on Dark Age Pisidia</i> .....	375
İzzet Duyar – Derya Atamtürk <i>Tlos (Seydikemer, Muğla) Kazılarında Ortaya Çıkartılan Orta Bizans Dönemi İskeletlerinde Ağız ve Diş Sağlığı</i> .....	405
Ebru Fındık <i>Bir Güzellik Nesnesi Olarak Cam Bilezikler: Demre/Myra Aziz Nikolaos Kilisesi Buluntuları (1989-2016)</i> .....	423
Güven Dinç <i>The Social and Economic Status of the Rum (Greeks) of Antalya in the First Half of the 19<sup>th</sup> Century</i> .....	449
<b>Book Review</b>	
Netice Yıldız <i>A New Book about Kyrenia, the Harbor Town of Cyprus</i> .....	491

## Unguentarium Production at Patara and a New Unguentarium Form: Archaeological and Archaeometric Interpretation

Erkan DÜNDAR – Ali Akın AKYOL\*

Recent excavations have yielded new evidence concerning unguentaria in Patara, requiring the addition of supplementary details to the typologies and chronologies discussed in a previous publication on the subject matter<sup>1</sup>.

Unguentaria are small, usually ceramic vessels thought to have contained oils and are commonly found throughout the necropoleis of the ancient world. The vessels display typologies that vary depending on their regions, which indicates that they were locally produced in almost every region rather than being produced in a single center. Although various types of unguentaria are known to exist, the fusiform (or spindle-shaped) unguentarium is the most common type<sup>2</sup>.

Several fragments of fusiform unguentaria interpreted as production waste were found in the excavations carried out at Patara in 2010, and their description constitutes the main motivation of this article (Fig. 8). Unearthed from the same layer as Rhodian-stamped amphora handles dating from the second half of the 2<sup>nd</sup> century BC and early 1<sup>st</sup> century B.C.<sup>3</sup> in the trenches along the waterway, these examples are to our knowledge the first production-waste unguentarium fragments to be found in Lycia, and at least the first ever to be published. These examples are of the typical Hellenistic fusiform style that accounts for the majority of the unguentaria found in Patara<sup>4</sup>. In general, examples of this typology feature a low-quality, porous clay tempered with sand granules and lime with a very thin coating, and a reddish-yellow or yellowish-red clay (5 YR 6/6, 6/8, 7/6, 7/8). Almost all fusiform unguentaria from Patara lack any amount of mica in their clay. The inner chambers of the examples, which tend to be

---

\* Assist. Prof. Dr. Erkan Dündar, Kahramanmaraş Sütçü İmam Üniversitesi, Fen – Edebiyat Fakültesi, Arkeoloji Bölümü, Aşağı Kampüsü 46100 Kahramanmaraş. E-mail: dundarerkan@gmail.com

Assist. Prof. Dr. Ali Akın Akyol, Gazi Üniversitesi, Güzel Sanatlar Fakültesi, Kültür Varlıklarını Koruma ve Onarım Bölümü 06830 Ankara. E-mail: aliakinakyol@gmail.com

We would like to thank J. M. Burgin for his assistance in the English editing of the manuscript.

<sup>1</sup> Dündar 2008, passim.

<sup>2</sup> Anderson-Stojanović 1987, 106-112, figs. 1-7; Dündar 2008, 3-4, 57-62.

<sup>3</sup> These Rhodian-stamped amphora handles include those manufactured by Moskhos II, known to have been active in Period V (ca. 145-108 B.C.), and Philokrates II, active in Period V-VI (ca. 145-88/86 B.C.), cf. Dündar 2017, 236 (Moskhos II), 242-243 (Philokrates II).

<sup>4</sup> About 800 examples of this type have been found at Patara, see Dündar 2008, 41.

sloppily made, are rather narrow. The vessels have a very elongated and completely solid foot, which makes them unable to stand upright on their bases without a support (Fig. 9). Ranging in size from 18 cm to 23 cm, almost all of the examples are grave finds<sup>5</sup>. In this regard, we can suggest a parallelism between the poor quality of these ceramics and their intended use. These unguentaria were probably intended for use as votive offerings or gifts for the dead left in burials, and not for daily use. This explains the cursory attention to production quality. The asymmetrical forms of some examples support this view (Fig. 10). The extensive use of the unguentaria in this typology at Patara during the 2<sup>nd</sup> century B.C., as well as the recently found production waste, confirms that they were locally produced vessels. In addition, the abundance of such examples in the necropolis sites points to the existence of a local workshop that could meet the demand in the city. The large amount of production waste unearthed in the trenches along the waterway should be considered as concrete evidence for the presence of an unguentarium workshop in Patara (?) that was active from at least the 2<sup>nd</sup> century B.C.

We should note that, besides the large numbers of fusiform unguentaria found in the city, several unguentaria of a different type also exist whose find contexts are dated to the late 1<sup>st</sup> century B.C. and 1<sup>st</sup> century A.D. This new type, which we call the “Eşen Type (spherical body)” due to its shape and the Eşen (Xanthos) Valley where it was first found, generally features a low and small base, a spherical body, and a long cylindrical neck terminating in a lip folded outward or inward (Fig. 11). Although the majority of the examples found in Patara are made of poorly fired clay, there are also finely fired examples too. Almost all examples feature a porous clay tempered with sand granules and lime. In some examples, the core of the clay grayed out due to substantial differences in temperature during the firing process. The examples with reddish-yellow/red clay are covered with a thin slip in the same color as clay or in a somewhat lighter color (light pink). The clay fabric structure of this new form shows features comparable to that of other fusiform unguentaria (production waste) found in the city. The similarities in clay of the fusiform and Eşen Type unguentaria, along with their intensive use in the Patara, is further indication for the presence of one or more local pottery workshops manufacturing unguentaria. Based on the available pottery production waste, we can suggest that the workshop(s) was active from at least the 2<sup>nd</sup> century B.C. and must have continued production activities well into the Early Roman Imperial period while undergoing only a slight change in form.

Eşen Type unguentaria had a regional distribution pattern. Lycian cities where we have found examples of Eşen Type unguentaria include Xanthos<sup>6</sup>, Letoon<sup>7</sup>, Tlos<sup>8</sup>, Andriake<sup>9</sup>, and Patara<sup>10</sup>. The only example of the type found outside of the Eşen Valley so far is a fragment recovered from Tomb A3 during the excavations in the Eastern Necropolis of Attaleia<sup>11</sup>. The

<sup>5</sup> Dündar 2008, 79-84, table 1, U84-109.

<sup>6</sup> Demargne 1958, pl. 15, no. 716.

<sup>7</sup> le Roy 2005, 259, fig. 16.

<sup>8</sup> Korkut – Işın 2015, 225, fig. 1, no. 4. The excavations at the acropolis in 2005 unearthed an intact Lycian rock-cut tomb. The excavations inside this tomb yielded several Eşen Type unguentaria with longer bases as compared to the examples found in other settlements, a feature different from those from Xanthos, Letoon, Andriake, and Patara. This information is derived from personal observations during the excavation of the rock-cut tomb, in which E. Dündar participated as an excavation team member

<sup>9</sup> Çevik – Bulut 2010, 108, fig. 145; Özdilek 2016, 229, 247-248, U7-8.

<sup>10</sup> İşkan-Yılmaz – Çevik 1995, fig. 7h; Dündar 2008, pls. 18-24, U145-190.

<sup>11</sup> Büyükyörük – Tibet 1999-2000, 160, fig. 13, A3/6.

Attaleian example, whose base and mouth are missing, has a long cylindrical neck rising on a spherical body.

The examples of Eşen Type unguentarium recovered from the five sites mentioned above share similar clay fabric properties and usually feature, as in the fusiform unguentaria found in Patara, a poorly fired, porous clay tempered with sand granules and lime, as well as a thin layer of slip applied in a very light color. The similarities in the forms and clay structure of the unguentaria from the five sites suggest that this type may have been produced and marketed by a single pottery workshop.

Some studies have mentioned this new type of unguentarium, which is of great importance for the region of Lycia, but it has otherwise remained mostly unnoticed. Ch. le Roy, for example, included in his study a comparison of the examples from Letoon with those found in Deposit G at the Athenian Agora<sup>12</sup>. However, the Athenian example diverges from this local type in many aspects, especially in its form<sup>13</sup>: It had a broken neck and base, and was reconstructed based on the model of Unguentarium F 49, included in Group F. Thus, such a comparison could not lead to a reliable conclusion<sup>14</sup>. Other studies have compared the Eşen Type of unguentarium to unrelated examples based only on certain characteristics, such as a bulbous body and a long cylindrical neck. A singular example found in the excavations at the necropolis of Laodicea roughly resembles the Eşen Type in the general outline of its form. However, the Laodicean example has the divergent characteristics of a sharp base profile, a hollow base ring, and a mouth edge folded outward, which makes its association with the Eşen Type impossible<sup>15</sup>. Instead, examples of the Eşen Type, which appear to feature a local form unique to the Lycian region in the Early Roman Imperial period, should be evaluated based on the comparisons with relevant finds from the region internally.

The unguentaria of the Eşen Type account for 13% of the over 1,000 examples from Patara that have been so far examined, thus constituting the second largest group of unguentaria after the fusiform group. This relatively high proportion indicates that such materials found intensive use at the site (Figs. 12-13)<sup>16</sup>. Another key finding supporting the idea that this type of unguentarium is a regional form is that Patara has so far yielded a very limited number of bulbous unguentaria<sup>17</sup>, a form which replaced the fusiform unguentaria throughout the eastern Mediterranean basin during the Late Hellenistic and Early Roman periods<sup>18</sup>. The abundance of the Eşen Type of unguentaria, in contrast to the scarcity of the bulbous type, signifies that Patara, unlike many other sites, relied mainly on locally produced vessels to satisfy the local demand during the Early Roman Imperial period, rather than imported unguentaria of the bulbous form (Figs. 12-13). Future research may prove a similar case for other sites in Lycia.

---

<sup>12</sup> le Roy 2005, 251, n. 29.

<sup>13</sup> Robinson 1959, pl. 5, G 96

<sup>14</sup> Robinson 1959, 31, pl. 2, F 49.

<sup>15</sup> Şimşek – Okunak – Bilgin 2011, 66-67, pl. 63, 8.

<sup>16</sup> Chronological data related to the unguentaria shown on Fig. 13 were derived from the following excavated areas in Patara: Tepecik Acropolis (end of the 4<sup>th</sup> century B.C.), Tepecik Necropolis (3<sup>rd</sup> century B.C.), underground chamber tombs (2<sup>nd</sup> century B.C.– 1<sup>st</sup> century A.D.), Harbor Bath and Harbor Street (5<sup>th</sup> – 7<sup>th</sup> century A.D.); see Dündar 2008, 11-37.

<sup>17</sup> The bulbous unguentaria account for 1% of over 1,000 examples so far examined.

<sup>18</sup> About this matter, see Anderson-Stojanović 1987, 110; Hayes 1997, 86; Dündar 2008, 24. This form, which first appeared in the 1<sup>st</sup> century B.C., became popular until the spread in the 1<sup>st</sup> century A.D. of glass unguentaria made by the blowing technique; see Hayes 1975, 29; Anderson-Stojanović 1992, 81.

For the time being, it is difficult to speak of a form development in the Eşen Type of unguentaria. Trivial differences like a fluted or smooth body, a wide or narrow base, a miniature or large size, and lips folded inward or outward might not indicate typological distinction within the type. Such small differences could have resulted from the individual rendering of the craftsman or workshop. Besides, the allocation of such small differences among the Eşen Type of unguentaria into their limited chronological timeline would be a complex task. For the type does not span an extended period of time, unlike the fusiform unguentaria. All examples recovered so far generally exhibit common features of a particular form, which may be attributed to the use of these ceramics within a limited period of time, to the fashion of the day, or to the rituals performed at the necropoleis.

All examples of the Eşen Type of unguentaria found at Patara were recovered in the necropolis areas (i.e., Günlük and Tepecik). As in the fusiform examples, we can suggest a parallelism between the poor quality of the materials and their intended use as grave goods<sup>19</sup>. The lack of elaboration in their production indicates that they were intended for use as votive offerings or gifts left in burials, and also points to a mass production activity. As with the fusiform examples, this view is further supported by the asymmetrical forms of some examples (Fig. 14). The concentrated presence of the Eşen Type of unguentaria in the necropoleis of the Eşen Valley points to a common social tradition or ritual for the region.

The first study on the subject suggested that the Eşen Type unguentaria was a local product manufactured at the sites located within the Eşen Valley<sup>20</sup>. The fusiform unguentaria recovered at Patara between 2009 and 2011, which were interpreted as production waste, yielded some new and important evidence in favor of this hypothesis. We conducted a series of archaeometric analyses on the fusiform unguentaria and the Eşen Type of unguentaria (both production waste and marketable products) found at Patara. A further archaeometric investigation involved a comparison of the results with the clay samples obtained from different areas of Lycia. The results of these analyses showed that the raw material used in the production of both the fusiform examples and the Eşen Type of unguentaria was obtained from the basin of the Eşen River.

## Archaeometric Studies

Through archaeometric research, the raw material characteristics of ceramic sherds can be defined and information reached about their production and firing technologies. To this end, unguentarium pieces retrieved from Patara were examined archaeometrically. Our aim was to demonstrate the local nature of production by comparing the ceramic sherds with clay samples taken from the surroundings of Patara.

Unguentarium sherds and clay samples<sup>21</sup> (Figs. 1-2, 15-18) were examined at Gazi University, Faculty of Fine Arts, Department of Restoration and Conservation of Cultural Properties, Historical Materials Research and Conservation Laboratory (MAKLAB) and University of Ankara, Earth Sciences Application and Research Center (YEBİM) by using the archaeometric methods discussed below.

<sup>19</sup> On use as a grave gift, see Thompson 1934, 472; Boulter 1963, 125, pl. 46, K 2; Åström 1964, 189; Knigge 1976, pl. 69, nos. 387, 6-7, 388, 390; Rotroff 1997, 176.

<sup>20</sup> Dündar 2008, 27-30.

<sup>21</sup> We would like to thank B. Ünlütürk for obtaining clay samples from various areas.



## Archaeometric Methods and Analyses

Eight unguentarium sherds retrieved from the excavations at Patara and eight clay samples from various parts of Lycia were analyzed through archaeological and archaeometric perspectives (Figs. 1-2, 17-18). These samples were first visually evaluated and classified, then coded and documented photographically by Canon Digital IXUS 870 IS 10 Mp (Figs. 1-3).

The clay colors of the unguentarium sherds were defined with a portable chroma meter using the program of ColorQA Pro System III with the standard CIE L\*a\*b\* color system (Fig. 3). The CIE L\*a\*b\* (Commission internationale de l'éclairage) color system is one of the most widely used and most detailed standard color systems for documentation, and helps overcome inaccurate color identifications resulting from subjective evaluation. (L) value represents the lightness value of the color, (+a) value represents the intensity of red in the color, (-a) value represents the intensity of green in the color, (+b) value represents the intensity of yellow in the color, and (-b) value represents the intensity of blue in the color<sup>22</sup>.

Petrographic textural (matrix) and aggregate (rock and mineral content) characteristics of ceramic and clay samples were identified through optical microscope analysis of thin section (Figs. 4-5, 19). The samples were prepared for optical microscope analysis by being cut with an appropriate cutter and placed onto the microscope slide. The thin sections were prepared

Fig. 1 Unguentaria samples from Patara

Unguentaria Samples	Descriptions
PK-B1	The fusiform unguentarium (production-waste) PTR'10 - waterway SU-33 (1)
PK-B2	The fusiform unguentarium PTR'89 Tlepolemos - U45 (2)
PK-B3	The fusiform unguentarium PTR'89 Tepecik Necropolis L.20B (3)
PK-B4	The fusiform unguentarium PTR'97 Günlük Necropolis, G34 - U478 (4)
PK-B5	The Eşen Type unguentarium PTR'95, Günlük Necropolis, G4 - U85 (5)
PK-B6	The Eşen Type unguentarium PTR'93 TG 3 - U460 (6)
PK-B7	The Eşen Type unguentarium, PTR'95, Günlük Necropolis, G1 - U1 (7)
PK-B8	The Eşen Type unguentarium, PTR'97, Günlük Necropolis, G42 - U186 (8)

Fig. 2 Clay samples from Lycia

Clay Samples	Descriptions
PK-D1	Vicinity of Karadere Village (near Letoon)
PK-D2	Vicinity of Elmalı (Testici Hasan Workshop)
PK-D3	River bank of Eşen near Kınık
PK-D4	Vicinity of Sura (Demre)
PK-D5	River bank of Kasaba Village (Kaş)
PK-D6	Near Geçmen Village clay deposits (Elmalı)
PK-D7	Vicinity of Hacimusalar Village
PK-D8	Near Esenköy (Dont) Village (Fethiye)

<sup>22</sup> Ohno 2007, passim.

Fig. 3 Chromametric (L\*a\*b) descriptions of the unguentaria and clay samples

Unguentaria Samples	Color Codes			Clay Samples	Color Codes		
	L	a	b		L	a	b
PK-B1	19,01	19,57	28,03	PK-D1	18,91	12,50	27,56
PK-B2	25,75	21,65	36,23	PK-D2	27,03	-0,48	26,88
PK-B3	22,62	20,56	32,57	PK-D3	29,77	-3,83	20,38
PK-B4	27,09	14,93	37,19	PK-D4	14,82	22,78	22,54
PK-B5	40,35	15,63	42,44	PK-D5	55,19	-8,22	27,44
PK-B6	24,21	11,44	33,86	PK-D6	38,19	-6,48	21,87
PK-B7	38,66	22,46	44,15	PK-D7	39,24	-2,03	32,31
PK-B8	43,88	26,74	48,28	PK-D8	31,16	2,51	22,41
Ave.	30,20	19,12	37,84	Ave.	31,79	2,10	25,18

Fig. 4 Thin section of optical microscopy analysis of unguentaria sherds

Unguentaria Groups	T (°C)	P (%)	Ag/Bin (%)	Rocks & Minerals*	Related Soil Groups
Ung. Gr1	950	12	2/98	Q, Ch, Pl, G, Pl, Op	Gr2
Ung. Gr2	800	6	42/58	Q, Ch, By, Cr, Op, K, BP (%15)	Gr5
Ung. Gr3a	800	6	32/68	Q, Ch, Pl, K, C, Py, By, Op, BP (2%)	?
Ung. Gr3b	800	5	35/65	Q, Ch, Pl, K, C, Py, By, Op, BP (2.5%)	Gr1
Ung. Gr4	900	3	15/85	Q, Ch, Op, BP (1.5%)	Gr5

(\*) B: Basalt, BP: Brick Particles, C: Calcite, Ch: Chert, Cr: Cerisite G: Granite, K: Limestone, O: Olivine, Op: Opaque Minerals, Pl: Plagioclase, Py: Pyroxene, Q: Quartz, R: Radiolarite

Groupings of Unguentarium Sherds

Ung. Gr1 : APT-B1

Ung. Gr2 : APT-B2 and APT-B3

Ung. Gr3a : APT-B4 and APT-B8

Ung. Gr3b : APT-B5 and APT-B6

Ung. Gr4 : APT-B7

Fig. 5 Thin section optical microscopy analysis of soil/clay samples

Clay Groups	Rocks & Minerals*	Sil/Clay Matrix
Clay Gr1	Q, Ch, Op	Illite + Smectite
Clay Gr2	Q, Pl	Illite + Carbonate
Clay Gr3	Q, Ch, Op	Illite + Carbonate
Clay Gr4	?	Illite + Iron oxide
Clay Gr5	Q, Op	Smectite + Carbonate

(\*) Ch: Chert, Op: Opaque Minerals, Pl: Plagioclase, Q: Quartz

Grouping of the soil/clay samples by the thin section analysis

Clay Gr1 : PK-D6 and PK-D8

Clay Gr2 : PK-D7

Clay Gr3 : PK-D5

Clay Gr4 : PK-D4

Clay Gr5 : PK-D1, PK-D2 and PK-D3

Fig. 6 The main and trace elemental composition of the clay/soil samples

Element	Conc.	PK-D1	PK-D2	PK-D3	PK-D4	PK-D5	PK-D6	PK-D7	PK-D8	Ave.
Na <sub>2</sub> O	%	0,070	0,073	0,074	0,072	0,074	0,075	0,077	0,770	0,161
MgO	%	1,98	3,61	12,46	0,71	7,94	7,03	5,10	4,41	5,41
Al <sub>2</sub> O <sub>3</sub>	%	9,90	9,15	5,92	21,88	6,19	8,30	6,84	17,10	10,66
SiO <sub>2</sub>	%	45,48	37,80	38,21	40,48	35,07	36,05	42,81	45,73	40,20
P <sub>2</sub> O <sub>5</sub>	%	0,127	0,106	0,070	0,812	0,086	0,080	0,100	0,135	0,189
SO <sub>3</sub>	%	0,179	0,147	0,351	0,175	0,129	0,476	0,171	0,121	0,218
Cl	%	0,000	0,000	0,007	0,001	0,004	0,004	0,002	0,011	0,004
K <sub>2</sub> O	%	1,39	1,57	0,84	0,84	0,99	1,71	1,09	0,17	1,07
CaO	%	13,12	15,56	15,16	1,04	17,86	16,32	13,47	6,02	12,32
TiO <sub>2</sub>	%	0,559	0,558	0,410	1,23	0,446	0,441	0,462	0,744	0,606
V <sub>2</sub> O <sub>5</sub>	%	0,015	0,017	0,017	0,034	0,019	0,015	0,018	0,038	0,022
Cr <sub>2</sub> O <sub>3</sub>	%	0,031	0,064	0,135	0,046	0,098	0,072	0,159	0,022	0,078
MnO	%	0,138	0,115	0,086	0,048	0,085	0,078	0,074	0,156	0,097
Fe <sub>2</sub> O <sub>3</sub>	%	4,53	6,01	5,94	11,64	5,51	5,79	4,23	10,52	6,77
LOI*	%	22,48	25,22	20,31	20,99	25,50	23,56	25,40	14,05	22,19
Co	ppm	36,2	65,9	65,1	68,5	26,5	54,1	35,1	57,7	51,1
Ni	ppm	107,5	260,2	605,9	175,1	462,9	395,6	233,7	121,4	295,3
Cu	ppm	36	33,6	26,7	28,5	24,9	30,4	20,6	101,4	37,8
Zn	ppm	66,3	73,5	50,8	126,8	50,9	75,9	43,6	60	68,5
Ga	ppm	11,6	15,8	8,3	34,7	9,9	14	10,2	17,3	15,2
Ge	ppm	0,9	1,5	0,6	2,1	1,3	1,3	1,2	1,3	1,3
As	ppm	8,4	5,2	4,7	11,6	4,7	4,9	5	0,5	5,6
Se	ppm	0,4	0,4	0,4	0,5	0,4	0,6	0,4	0,4	0,4
Br	ppm	9,1	2,9	1,2	7,4	5,7	2,2	1,4	2,1	4,0
Rb	ppm	57,4	72,2	30,8	73,4	37,3	67,8	37,4	1,9	47,3
Sr	ppm	67,6	221,6	229,4	428	248,9	461,7	201,8	135	249,3
Y	ppm	43,4	17,9	12,7	69,2	12,8	15,6	12,1	26,7	26,3
Zr	ppm	125,8	104,1	79,6	378,8	74,7	95,3	126	71,3	132,0
Nb	ppm	11,1	9,5	9,2	39	5,3	7,8	10	4,8	12,1
Mo	ppm	3,3	3,3	3,4	4,1	3,2	3,9	2,5	3,1	3,4
Cd	ppm	0,9	0,8	0,9	1,9	0,9	1	0,9	0,9	1,0
In	ppm	0,8	0,7	0,8	0,8	0,8	0,9	0,8	0,9	0,8
Sn	ppm	0,7	1,8	1,1	4,8	1,8	2,2	1,9	1,8	2,0
Sb	ppm	1	0,9	0,6	1,1	0,5	1,8	0,9	0,9	1,0
Te	ppm	1,3	1,2	1,2	1,3	1,2	1,4	1,3	1,3	1,3
Cs	ppm	3,7	3,8	4,7	5,1	4,5	4	6,2	7,4	4,9
Ba	ppm	193,8	247,4	147,7	320	147,7	525	192,2	44,8	227,3
La	ppm	42,8	24,7	16,1	83,5	15	18,6	7,8	17,1	28,2

Element	Conc.	PK-D1	PK-D2	PK-D3	PK-D4	PK-D5	PK-D6	PK-D7	PK-D8	Ave.
Ce	ppm	45,2	58,1	23,6	144,6	33,6	39,7	39,3	14,6	49,8
Hf	ppm	5,2	5,3	5,4	6	5,2	5,5	4,6	8,6	5,7
Ta	ppm	6,1	7	8,5	7,2	8	7,7	6	10	7,6
W	ppm	4,7	6,1	8,2	6,5	7,7	7,4	5,7	5,5	6,5
Hg	ppm	1,2	1,4	1,3	1,4	1,3	1,3	1,2	1,4	1,3
Tl	ppm	0,7	1,5	1,3	1,9	1,4	1,4	1,2	1,4	1,4
Pb	ppm	15,6	13,3	7,2	37,3	6,3	13,6	8,1	0,9	12,8
Bi	ppm	0,9	1	1	1,3	0,9	1	0,5	1	1,0
Th	ppm	7,3	5,8	1	19,7	0,9	0,5	1,1	1,4	4,7
U	ppm	9,1	7,4	7,6	9,1	17	9,6	7,4	7,5	9,3

(\*) LOI: Loss on Ignition at 950°C

Fig. 7 The main and trace elemental composition of the unguentarium sherds

Element	Conc.	PK-B1	PK-B2	PK-B3	PK-B4	PK-B5	PK-B6	PK-B7	PK-B8	Ave.
Na <sub>2</sub> O	%	0,087	0,087	0,087	0,096	0,090	0,320	0,086	0,084	0,117
MgO	%	2,56	3,36	2,72	1,33	6,20	4,16	6,87	3,80	3,88
Al <sub>2</sub> O <sub>3</sub>	%	12,05	10,76	1,79	10,88	9,93	9,61	12,48	11,35	9,86
SiO <sub>2</sub>	%	39,19	42,48	10,22	43,01	42,89	43,12	47,89	43,77	39,07
P <sub>2</sub> O <sub>5</sub>	%	0,142	1,266	0,142	9,321	0,190	0,197	0,138	0,298	1,46
SO <sub>3</sub>	%	0,184	0,207	0,158	0,125	0,248	0,290	0,190	0,209	0,201
Cl	%	0,042	0,061	0,029	0,022	0,116	0,120	0,065	0,117	0,071
K <sub>2</sub> O	%	1,82	1,83	0,38	1,51	1,61	1,52	2,11	1,60	1,55
CaO	%	6,13	6,90	52,01	8,79	10,60	7,38	10,00	5,88	13,46
TiO <sub>2</sub>	%	0,784	0,669	0,172	0,671	0,664	0,617	0,754	0,725	0,632
V <sub>2</sub> O <sub>5</sub>	%	0,028	0,020	0,006	0,023	0,024	0,035	0,032	0,027	0,024
Cr <sub>2</sub> O <sub>3</sub>	%	0,070	0,061	0,038	0,058	0,066	0,048	0,063	0,064	0,058
MnO	%	0,141	0,154	0,053	0,089	0,126	0,164	0,113	0,117	0,120
Fe <sub>2</sub> O <sub>3</sub>	%	8,57	7,77	2,05	7,11	8,21	7,28	8,62	8,14	7,22
LOI*	%	28,20	24,37	30,15	16,96	19,02	25,14	10,59	23,82	22,28
Co	µg/g	71,6	56,9	19	37,6	73,4	95	39	44,8	54,7
Ni	µg/g	312,9	337,5	149,3	183,6	453,4	394,4	426,9	370,3	328,5
Cu	µg/g	42,8	187,3	90,7	43,7	46,6	79,5	44,3	47,7	72,8
Zn	µg/g	109,2	144,4	63,9	124	94,1	93,9	92,9	100,3	102,8
Ga	µg/g	22,3	18,3	5,7	19,3	16,4	16,3	18,2	18,8	16,9
Ge	µg/g	1,4	1,4	0,8	1,2	1,1	1,5	0,7	0,8	1,1
As	µg/g	9,4	8,7	3,3	2,2	4,8	13,3	3,8	4,6	6,3
Se	µg/g	0,5	0,5	0,6	0,5	0,5	0,4	0,5	0,5	0,5
Br	µg/g	3,8	3,2	6	2,8	4,7	7,9	2,7	3,1	4,3
Rb	µg/g	104,5	81,8	17,2	64,4	76,7	74,1	98,2	79,2	74,5

Sr	µg/g	169,3	254,7	319,1	570,4	231,3	202,6	289,4	143,6	272,6
Y	µg/g	33,8	23,2	5,7	23,4	22,5	17,3	23	23	21,5
Zr	µg/g	247,6	167,9	94,7	143	140	126,9	140,8	163,2	153,0
Nb	µg/g	22,4	16,6	6,5	17,9	13,4	13,4	13,4	15,6	14,9
Mo	µg/g	5,7	5,2	4,5	3,5	5,2	3,7	3,3	3,5	4,3
Cd	µg/g	1,3	1	1,2	0,9	1	0,9	0,9	0,9	1,0
In	µg/g	1,1	1	1,3	0,9	1	0,9	0,8	0,9	1,0
Sn	µg/g	3,5	15,2	3,6	4,6	3,5	2,8	3,7	2,6	4,9
Sb	µg/g	1,4	1,2	1,4	2	1,1	0,8	0,9	1,1	1,2
Te	µg/g	1,9	1,7	1,2	1,3	1,5	1,2	1,3	1,5	1,5
Cs	µg/g	9,3	4,7	5,5	3,4	6,1	4,1	6,4	10,8	6,3
Ba	µg/g	352,1	614,9	163,1	295,6	291,4	365,2	325,5	354,5	345,3
La	µg/g	63,7	23,5	18,2	31,8	35,3	30,2	26	37,9	33,3
Ce	µg/g	107	60,3	35,8	59,5	63,2	48,5	57	56,3	61,0
Hf	µg/g	5,2	10	8,6	6,1	6,2	7,4	6,9	6,5	7,1
Ta	µg/g	8,3	13	11	7,5	9	9,8	9,3	9,1	9,6
W	µg/g	7,7	8	6,6	6,3	8	7,4	8,2	7,8	7,5
Hg	µg/g	1,5	1,4	1,6	1,4	1,4	1,3	1,6	1,1	1,4
Tl	µg/g	1,7	1,6	1,8	1,6	1,6	1,5	1,8	1,7	1,7
Pb	µg/g	34	50,2	42,7	34,8	48,2	30,7	43,6	37,1	40,2
Bi	µg/g	1,2	0,7	1,4	1,1	1,2	0,4	1,2	1,1	1,0
Th	µg/g	11,3	5,9	1,5	6,3	5,1	3,4	6,1	6	5,7
U	µg/g	7,8	6,9	18,7	7,6	9,9	7,7	8	7,1	9,2

(\*) LOI: Loss on Ignition at 950°C

by thinning them<sup>23</sup>. Thin sections of the samples were examined by using the optical microscope LEICA Research Polarizing Microscope DMLP Model with illumination from both below and above. Photographs were taken with Leica DFC280 digital camera attached to the microscope (on single and double nicols with appropriate magnification), and the evaluations were made by using Leica Qwin Digital Imaging Software. The matrix in the samples and the clay, rock, and minerals that constitute the matrix were identified by using Point Counting Method<sup>24</sup>.

The chemical compositions of the ceramic and clay samples were attained through PED-XRF analysis (Figs. 6-7, 20 a-b). In the analysis a SPECTRO X-Lab 2000 PEDX brand spectrometer working with a Polarized Energy Dispersive (PED-XRF) system was used. After pulverizing the analysis samples selected for the analysis in an agate mortar, 32 mm discs were formed. Each disc was mixed with a chemical (wax) used in the XRF analysis, placed on the sample stage of the device, and analyzed. The sensitivity threshold of the device is 0.5 ppm for heavy elements and 10 ppm for light elements. In this study, around 50 main/trace elements could be identified. Because of the weight loss due to the high temperature (950 °C) applied within the

<sup>23</sup> Whitebread 1995, 365.

<sup>24</sup> Kerr 1977, *passim*; Rapp 2002, *passim*.

scope of the analysis, lithium, boron, and fluorine cannot be detected. Major and minor elements in the analysis are expressed in the form of oxide percentages (%) and trace elements are given in one in a million (ppm) concentration. In the analysis, USGS (U.S. Geological Survey) standards and as for references GEOL, GBW-7109, and GBW-7309 were used<sup>25</sup>.

## Discussions and Assessments

Sherds of ceramic unguentarium from Patara archaeological site and clay samples sampled from different regions of Lycia were examined archaeometrically. The results are presented here (Figs. 1-7, 15-21a-c).

The clay colors of the sherds vary according to raw materials and firing characteristics. The color codes of the samples were documented with the CEI L\*a\*b\* color code system. In the ceramic sherds (L) color code value varies between 19.01 and 43.88 (avg. 30.20), (a) color code value varies between 11.44 and 26.74 (avg. 19.12), and (b) color code value varies between 28.03 and 48.28 (avg. 37.84) (Figs. 3, 15, 16).

The clay samples (L) color code value varied between 14.82 and 55.19 (avg. 31.79), (a) color code value varies between -0.48 and -22.78 (avg. 2.10), and (b) color code value varies between 20.38 and 32.31 (avg. 25.18) (Figs. 3, 17).

Clay samples from different regions that were analyzed petrographically were obtained from clay deposits still in use today. Clay samples sampled from eight different locations were classified in terms of matrix (clay type) and aggregated in five groups, and associated with the examined ceramic unguentarium sherds (Fig. 4). Petrographic and mineralogical characteristics of the clay samples demonstrated that they have a matrix texture and structure in illite, smectite, carbonate, and iron oxide types, and in the form of various mixtures (smectite+carbonate, illite+iron oxide, illite+carbonate, and illite+smectite).

With thin section analysis aiming to achieve petrographical data about the production of unguentarium in Patara, the aggregate and matrix structures of the sherds were defined in detail and associated with the clay samples on hand. The petrographically examined ceramic samples were classified in terms of their matrix (clay) structure, porousness, aggregate ratio, type, and dispersion in four main groups with two subgroups (Figs. 5, 19). In the most general sense, the level of variation of the ceramics constituting the sample set varied considerably, indicating either that a homogeneous/standard production did not exist within them or that the production approach used multiple origins of different raw material.

The existence of carbonate containing aggregates (limestone, travertine, marble, etc.), the clay structure being preserved, the intensity of porousness, or the existence of large pores indicate that firing took place at low temperatures (<800°C). Above this, at 900°C and higher, the matrix clay structure of ceramics degenerate in firings and undergo a glass transition (vitrification). In the samples tested, the firing temperature varied between 800°C and 900°C. All samples except for the very low-fired sample Ung. Gr1 were subject to firing at low (800-850°C) or (900°C) average temperatures. Among the samples Gr2, Ung. Gr3a, and Ung. Gr3b samples had been subject to firing at lower temperatures (800-850°C). Other samples had been subject to firing at average (~900°C) and higher (>900°C) temperatures (Fig. 6).

---

<sup>25</sup> Shackley 2011, 7-44.

The unguentarium sherds had a porous structure (porousness) at ratios ranging from 3 to 12%. Compared to other sherds, the sample labelled as Ung. Gr1 (PK-B1) has a more porous structure (12%).

Unguentarium sherds were associated with clay sample groups on hand according to their matrix characteristics (Figs. 4, 5). The samples were mostly illite, at lower ratios smectite, and carbonate (containing iron oxide) group clays. The existence of a high level of smectite type in the clay leads to characteristics of plasticity showing expansion beginning from low temperatures and not being suitable during firing. Among the sherds the Ung. Gr3a sample could not be associated with any clay group on hand, having different characteristics from the examined clay groups (Fig. 5). The ceramic samples have the highest coherence with Clay Gr1 from the group, Karedere-Elmalı-Eşen regions (Fig. 2).

When the unguentarium sherds were evaluated in terms of their matrix aggregate content, it was detected that the total matrix aggregate ratio of the samples varied between 2% and 42%. It was detected that the matrix structures of the samples were formed by aggregates at different ratios, yielding a heterogeneous dispersion, in angular form and in different kinds and sizes (Figs. 5, 19). The raw material content of the samples was prepared by crushing, and with local angular rock brush in different sizes and exhibiting a heterogeneous dispersion.

Among the unguentarium sherds, in the aggregate content of the sample groups, except Ung Gr1, brick brush (at ratios from 1.5% up to 15% of the total aggregate) was also encountered (Fig. 5). It is not possible to set forth an exact opinion about whether the brick brush detected in the samples had been added to the aggregate content on purpose during the production or indicate an accidental uncontrolled mixing/contamination. However, it is likely the brick brush detected in varying ratios in most of the samples indicated a deliberate choice.

The various petrographic and chemical characteristics of the clays used in the production centers, obtained from local stream beds in a refined form, provide endurance with their various features (features of plasticity, ease of firing/production, coloring, etc.) and are thus rather significant for ceramic production. Different from the type of the clay, the aggregates constituting the clay structure provide important information about the origins of the production centers by naturally including compounds reflecting the rock structure of the region. Among the ceramics of the tested sherds, the aggregates that reflect the weathering of different kinds of rocks (volcanic minerals and rocks such as granite, pyroxene, etc.) had characteristics found in clays distant from the sea and closer to the stream beds washing off the rock groups. This condition indicates that at least some of the samples (i.e., Ung. Gr1/Clay Gr5) do not reflect the environment in which they were found. In the light of the petrographical data, it seems mostly local clay resources (the Eşen River and its surroundings) were used as resource of the ceramics' raw material.

The chemical compositions of the unguentarium sherds from Patara and clay samples were reached through PED-XRF analysis (Figs. 6, 7, 21a-c). When the clay samples were evaluated in terms of their chemical compositions, it was seen that the contents of the main elements (> 1%) were constituted, at decreasing ratios, by: SiO<sub>2</sub> (35.07-45.73%; avg. 40.20%), LOI/total carbonate (LOI: Loss on Ignition/950°C, 14.05-25.50%; avg. 22.19%), CaO (1.04-17.86%; avg. 12.32%), Al<sub>2</sub>O<sub>3</sub> (5.92-21.88%; avg. 10.66%), Fe<sub>2</sub>O<sub>3</sub> (4.23-11.64%; avg. 6.77%), MgO (0.71-12.46%; avg. 5.41%) and K<sub>2</sub>O (0.17-1.71%; avg. 1.07%) (Fig. 6). The analyzed clay samples show considerably varying chemical contents based on the locations they were sampled. Among the samples, PK-D8 and especially PK-D4 are the ones which prominently differ from other samples in

their main and trace elemental content (Figs. 20a-b). The chemical analyses of the clay samples demonstrated that among the clay samples driven from different clay beds, two samples, namely PK-D4 (sampled from Sura) and PK-D8 (sampled from Dont), formed one group and the other samples a further, separate group (Figs. 20a-b).

When the unguentarium sherds were evaluated, we learned that the sherds had varying chemical compositions (Figs. 7, 21a-c). In terms of their chemical compositions, it was seen that the contents of the main elements ( $> 1\%$ ) were constituted, at decreasing ratios, by:  $\text{SiO}_2$  (10.22-47.89%; avg. 39.07%), LOI/total carbonate (10.59-30.15%; avg. 22.28%), CaO (5.88-52.01%; avg. 13.46%),  $\text{Al}_2\text{O}_3$  (1.79-12.48%; avg. 9.86%),  $\text{Fe}_2\text{O}_3$  (2.05-8.62%; avg. 7.22%), MgO (1.33-6.87%; avg. 3.88%) and  $\text{K}_2\text{O}$  (0.38-2.11%; avg. 1.55%) (Fig. 7). Within the samples, phosphate ( $\text{P}_2\text{O}_5$ ) content of the sample PK-B4 was significantly (up to 20 times) higher than other samples, in a way to reflect an impact at a higher level than an environmental impact. In general sense, the chemical contents of the samples have similar elemental ratios; however, the main elemental content of the sample PK-B3 had a considerably different structure from other sherds (Fig. 7). When the ceramic sherds were grouped according to their elemental contents, it was seen that the samples PK-B7 demonstrated a relatively close and the sample PK-B3 demonstrated a rather distant relation (Figs. 21a-c). The PK-B3 sample diverged prominently in its structure from the whole group.

When the ceramic samples were examined on the basis of contemporary ceramics (vessels, bricks, tiles, pipes, etc.), the resistance characteristics of the samples can be indirectly evaluated through the chemical contents identified by PED-XRF analysis. For the samples having a high level of physical resistance, their structures must contain  $\text{SiO}_2$  at a rate above 30% (in the samples avg. 39.07%), CaO at a rate below 10% (in the samples except PK-B3 avg. 7.95%) and  $\text{Fe}_2\text{O}_3$  at a rate below 8% (in the samples avg. 7.22%)<sup>26</sup>. As to the compatibility of the samples with the referred values,  $\text{SiO}_2$  contents show a high level of compatibility, and CaO and  $\text{Fe}_2\text{O}_3$  contents show compatibility at relatively limited rates (Fig. 7). Considering the function of the unguentaria which were used as containers for carrying commercial commodities, it is possible to say that their resistances are at an average rate.

In the production of ceramic, elements of strontium (Sr) and zirconium (Zr) can give an idea about whether the raw material has a terrestrial or a marine source<sup>27</sup>. Strontium, being more than 400 ppm in the content of the sand used in the production of the ceramics, indicates that the clay obtained from marine sediments was used in the production. Strontium amounts in the terrestrial sands containing limestone are generally less than 150 ppm. Moreover, in the case of terrestrial sand being used in production, zirconium is expected to be more than 160 ppm. Respectively contents of Sr and Zr of the analyzed ceramic sherds are 272.6 and 153.0 ppm in average values (Fig. 7). All of the samples within the sample set, except PK-B4, must have been produced by using a clay with intensive terrestrial characteristics. The sample PK-B4 has a marine-based clay content with Sr: 570.4 ppm and Zr: 143 ppm. In addition, among the analyzed terracotta samples, the Strontium content of the samples PK-D4 and PK-D6 are 428 ppm and 461.7 ppm respectively (Sr avg. in terracotta 249.3 ppm), Zr contents are 378.8 ppm and 95.3 ppm (Zr avg. in terracotta 132.0 ppm) respectively (Fig. 7). These aforementioned terracotta samples must have a marine origin with their Sr and Zr contents.

<sup>26</sup> Özışık 2000, passim.

<sup>27</sup> Freestone et al. 2003, 19-32.



## Results

Eight unguentarium sherds retrieved from Patara and eight clay samples collected from different locations in Lycia were examined archaeometrically. Within the scope of the examination, the samples were classified according to the type of their material (sherd or clay sample), their sampling origin, and their physical characteristics (body clay colors), then documented photographically.

Through the optical microscopy analysis of thin section, the unguentarium samples were classified in four main groups and two sub-groups according to their matrix/aggregate content, aggregate type/dispersion/size, porousness, and characteristics of their clay (matrix) structures. Firing temperatures of the ceramics were mostly at 800-900°C. The matrix clay type of the samples was mostly composed of illite and smectite, and with some carbonate and iron oxide, or mixtures of these clays. In the aggregate content of most of the samples, brick brash was also detected, likely as a result of production. The petrographical quality of all of the samples, except PK-B3, have a structure in compliance with the local clay formations. The content of raw materials of the samples were prepared by crushing and with angular local rock brash chosen without a specific selection.

In terms of their chemical contents the samples have great similarities both among themselves and with the local soil in addition to their petrographical characteristics. In the local ceramic production terrestrial clays and the clays of the nearby stream bed (Eşen River Basin) must mostly have been used as a raw material resource.

According to the PED-XRF analysis results, the clay samples, except PK-D4 and PK-D8, have relatively similar chemical contents. The tile samples classified in four groups with their petrographical structures could be classified as a relatively homogenous single group (except PK-B3 and PK-B7) through PED-XRF analysis as well. In general sense, the samples reflect the structure of the local rocks.

The archaeometric analyses of the limited number of unguentarium sherds belonging to different locations in Patara enabled us to obtain important information. It will be possible to reach more comprehensive knowledge through examining Pataran unguentaria on a local and regional basis by increasing their numbers and diversifying them. Thus, it will be possible to determine whether Patara was a local center of ceramic production both for unguentaria and other ceramic genres. We will also learn about the city's range and technology of production and its relations to other production centers, as well as its connection to trade routes.

## Abbreviations and Bibliography

- Anderson-Stojanović 1987  
V. R. Anderson-Stojanović, “The Chronology and Function of Ceramic Unguentaria”, *AJA* 91, 1987, 105-122.
- Anderson-Stojanović 1992  
V. R. Anderson-Stojanović, *Stobi, The Hellenistic and Roman Pottery* (1992).
- Åström 1964  
P. Åström, “Two Unguentaria and an Obol”, *Opuscula Atheniensi* 7, 1964, 187-190.
- Boulter 1963  
C. G. Boulter, “Graves in Lenormant Street, Athens”, *Hesperia* 32, 1963, 113-137.
- Büyüköyük – Tibet 1999-2000  
F. Büyüköyük – C. Tibet, “1998-1999 Yılı Antalya Doğu Nekropolü Kurtarma Kazıları”, *Adalya* 4, 1999-2000, 115-171.
- Çevik – Bulut 2010  
N. Çevik – S. Bulut, “Myra ve Limanı Andriake”, in: N. Çevik (ed.), *Arkeolojisinden Doğasına Myra/Demre ve Çevresi* (2010) 25-115.
- Demargne 1958  
P. Demargne, *Les piliers funéraires* (1958).
- Dündar 2008  
E. Dündar, *Patara Unguentariumları*, Patara IV.1 (2008).
- Dündar 2017  
E. Dündar, *Transport Jars and Stamped Amphoras from Patara, 7th to 1st centuries BC. The Maritime Trade of a Harbor City in Lycia*, Patara IV.3 (2017).
- Freestone et al. 2003  
I. C. Freestone – K. A. Leslie – M. Thirlwall – Y. Gorin-Rosen, “Strontium Isotopes in the Investigation of Early Glass Production: Byzantine and Early Islamic Glass from the Near East”, *Journal of Archaeometry* 45, 1, 2003, 19-32.
- Hayes 1975  
J. W. Hayes, *Roman and Pre-Roman Glass in the Royal Ontario Museum* (1975).
- Hayes 1997  
J. W. Hayes, *Handbook of Mediterranean Roman Pottery* (1997).
- İşkan-Yılmaz – Çevik 1995  
H. İşkan-Yılmaz – N. Çevik, “Die Gräfte von Patara”, *Lykia* 2, 1995, 187-216.
- Kerr 1977  
P. F. Kerr, *Optical Mineralogy* (1977).
- Knigge 1976  
U. Knigge, *Der Südhügel, Kerameikos IX* (1976).
- Korkut – Işın 2015  
T. Korkut – G. Işın, “Fethiye Müzesinden Bir Grup Tlos Seramiği”, in: T. Korkut (ed.), *Arkeoloji, Epigrafi, Jeoloji, Doğal ve Kültürel Peyzaj Yapısıyla Tlos Antik Kenti ve Teritoryumu* (2015) 213-227.
- le Roy 2005  
Ch. le Roy, “La nécropole du Létoon de Ksanthos”, in: H. İşkan – F. Işık (eds.), *Güneybatı Anadolu’da Mezar Tipleri ve Ölü Kültü, Uluslararası Kolokyum, Antalya, 4-8 Ekim 1999*, *Lykia* 6 (2005) 247-260.
- Ohno 2007  
Y. Ohno, “Spectral Color Measurement”, in: J. Schanda (ed.), *CIE Colorimetry: Understanding the CIE System*, Ch. 5 (2007) 5.1-5.30.
- Özdilek 2016  
B. Özdilek, “2009-2012 Andriake Kazılarında Ele Geçen Unguentarium, Şişe, Lykion ve Mortar Örnekleri”, *Olba* 24, 2016, 217-265.
- Özışık 2000  
G. Özışık, *Yapı Mühendisliğinde Tuğla Elemanlar ve Yapı Sistemleri* (2000).
- Rapp 2002  
G. Rapp, *Archaeomineralogy* (2002).
- Robinson 1959  
H. S. Robinson, *Pottery of the Roman Period: Chronology* (1959).
- Rotroff 1997  
S. I. Rotroff, *Hellenistic Pottery Athenian and Imported Wheelmade Table Ware and Related Material* (1997).
- Shackley 2011  
M. S. Shackley, “An Introduction to X-Ray Fluorescence (XRF) Analysis in Archaeology”, in: M. S. Shackley (ed.), *X-Ray Fluorescence Spectrometry (XRF) in Ge archaeology* (2011) 7-44.

Şimşek – Okunak – Bilgin 2011

C. Şimşek – M. Okunak – M. Bilgin, Laodikeia Nekropolü (2004-2010 yılları), Laodikeia Çalışmaları 1.1/1.2 (2011).

Thompson 1934

H. A. Thompson, “Two Centuries of Hellenistic Pottery”, *Hesperia* 3, 1934, 311-480.

Whitbread 1995

I. K. Whitbread, *Greek Transport Amphorae: A Petrological and Archaeological Study* (1995).

## Özet

### Patara'da Unguentarium Üretimi ve Yeni Bir Unguentarium Formu: Arkeolojik ve Arkeometrik Yorum

Patara'nın unguentarium tipolojisi ve kronolojisinin ele alındığı çalışmanın yayınlanmasının ardından ulaşılan yeni veriler, konu hakkında tamamlayıcı niteliğe sahip bu makalenin ele alınmasına olanak tanımıştır. 2009 yılında gerçekleştirilen kazı çalışmalarında bulunan üretim atığı iç formlu unguentarium parçaları makalenin ana çıkış noktasını oluşturmaktadır.

Antik dünyada, özellikle nekropolislerde sıkça karşılaşılan unguentarium'ların bölgelere göre değişen farklı tipolojileri onların tek bir merkezden ziyade, hemen hemen tüm bölgelerde yerel olarak üretilmiş olduklarını göstermektedir. Farklı birçok tipi bilinen unguentarium'lardan iç formlu örnekler ise en çok karşılaşılan tip olarak karşımıza çıkar.

Patara'da MÖ 4-1. yy.'larda yoğun olarak görülen unguentarium formu iç formlu unguentarium'lardır. Bu formun ardından kentte en sık görülen ve buluntu kontekstleri MÖ 1. yy. sonu ve MS 1. yy. içlerine tarihlendirilen farklı tipolojideki unguentarium'lar ise dikkat çekicidir. Likya Bölgesi'nde yoğun olarak görüldüğü yerin Eşen (Ksanthos) Vadisi olmasından hareketle bu yeni form için "Eşen Tipi" isimlendirmesi tercih edilmiştir. Bu form, genelde alçak ve küçük çaplı kaideye, küresel gövdeye ve dışa çekik ya da içe dönük dudakla sonlanan uzun silindirik boyuna sahiptir. Genelde kırmızimsı sarı/kırmızı hamura sahip örneklerin hamurlarıyla aynı ya da daha açık (açık pembe) renkte uygulanmış ince astarları bulunur. Bu yeni formun hamur yapısı, kentte bulunan üretim atığı iç formlu örneklerle paralellik gösterir. Her iki tipolojideki örneklerin hamurları arasındaki benzerlik ve kentteki yoğun kullanımları unguentarium da üreten bir ya da birden fazla seramik atölyesinin varlığına işaret eder. Ele geçen üretim atığı parçalar ile en azından MÖ 2. yy.'da faal olan atölye ya da atölyelerin bu üretimlerine erken Roma İmparatorluk Dönemi'nde sadece form değiştirerek devam etmiş olduklarını söylemek mümkündür.

Konu üzerine yapılan ilk çalışmada, gözlemlere ve arkeolojik bulgulara dayanarak Eşen Tipi unguentarium'ların Eşen Vadisi'nde bulunan kentlerde üretilmiş olabileceği belirtilmiştir. Son yıllarda yapılan çalışmalarda ele geçen üretim atığı iç formlu örnekler ise, Eşen Tipi unguentarium'ların üretim yeri için önemli yeni verilere ulaşılmasına olanak tanımıştır. Kentte bulunan üretim atığı olan ve olmayan iç formlu unguentarium'lar ile Eşen Tipi unguentarium'lar arasından seçilerek incelemeye alınan örnekler fiziksel özellikleri açısından belgelendikten sonra arkeometrik yönden uygulanan petrografik ve kimyasal metotlarla ele alınmıştır. Ayrıca bu örneklerin hammadde kökenlerinin anlaşılabilmesi amacıyla da Patara'ya yakın, çoğunluğu Eşen Çayı havzasında yer alan farklı yörelerden örneklenen killere de ilişkilendirilmeye çalışılmıştır.

İnce kesit optik mikroskop analizi ile unguentarium'lar petrografik özelliklerine göre biri alt grup içeren 4 ana grup altında sınıflandırılmıştır. Örneklerin pişirim sıcaklıkları 800-950°C arasındadır. Seramik örneklerin yapısını; illit/smektit, illit/karbonat ve smektit/karbonat içeren ve 6 farklı yöreden örneklenen kil örneklerle ilişkilendirilebilecek mineral ve kayaçlar oluşturmaktadır. Seramiklerden Ung. Gr3a grubu örneklerinin, örneklenen kil kaynaklarının petrografik özelliklerinden farklı bir matriks yapısına sahip olduğu anlaşılmıştır. İncelenen iki grup kil kaynağı da seramik örneklerle ilişkilendirilememiştir. Örnek seti içindeki örneklerin çoğunun agrega içeriğinde tuğla kırığı parçaları da belirlenmiştir.

PED-XRF analizi uygulanan unguentarium örnekler, ana bileşenleri açısından nispeten birbirine benzer kimyasal içeriğe ve bununla beraber benzer üretim teknolojisine sahipse de,  $\text{SiO}_2$  /  $\text{Al}_2\text{O}_3$  ve kil grubu element dizinleri açısından en az 3 farklı atölye üretimini işaret eden kimyasal içerik sunmaktadırlar. Seramiklerin Sr ve Zr içeriklerinin ışığında üretimlerinde çoğunlukla (PK-B4 dışında) karasal kökenli hammadde kullanılmış olmalıdır.



Fig. 8 Production-waste unguentarium fragment, Patara.



Fig. 9 Fusiform unguentarium, Patara.



Fig. 10 Example of asymmetrical fusiform unguentarium, Patara.



Fig. 11 Unguentarium of Eşen Type (spherical body), Patara.

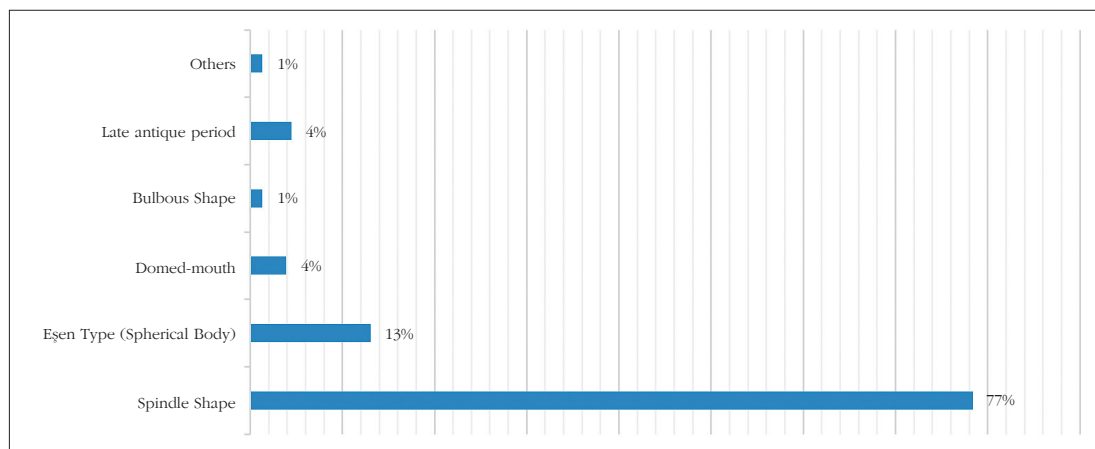


Fig. 12 Statistical distribution of forms of unguentaria at Patara.

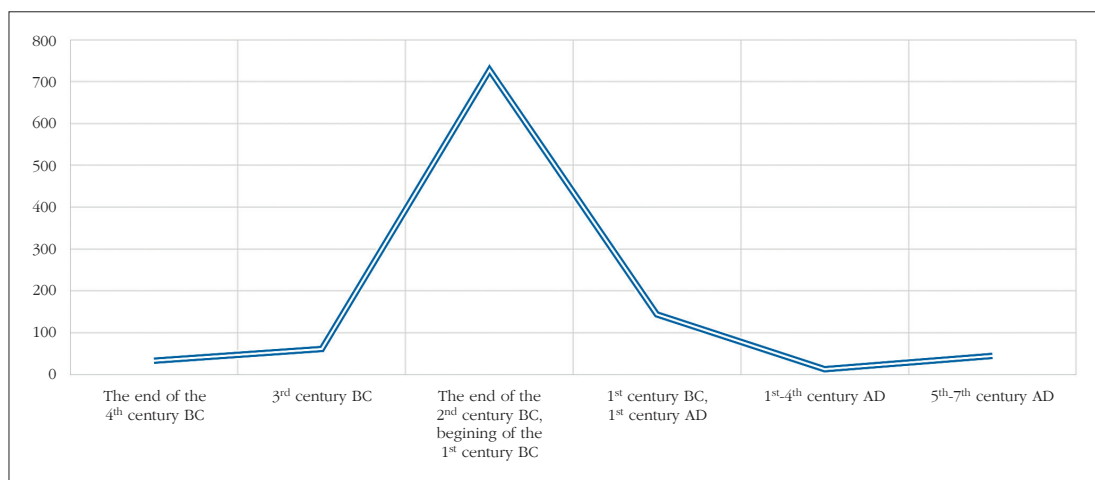


Fig. 13 Diagram showing chronological usage of unguentaria in Patara.

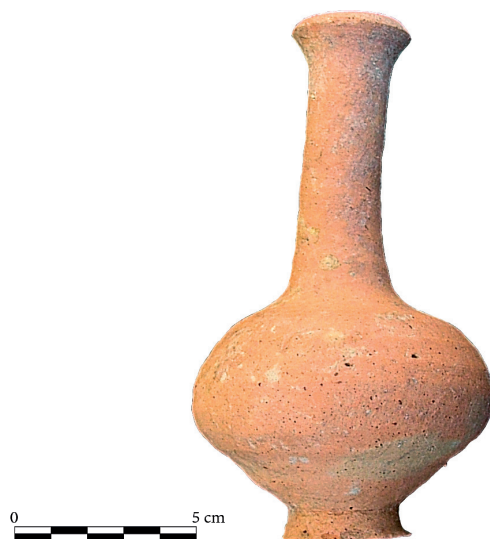


Fig. 14 Unguentarium of asymmetrical Eşen Type (spherical body), Patara.



Fig. 15 Analyzed unguentarium sherds, Patara.



Fig. 16 Analyzed unguentarium sherds, Patara.





Fig. 17 Soil-clay samples taken from different locations in Lycia.

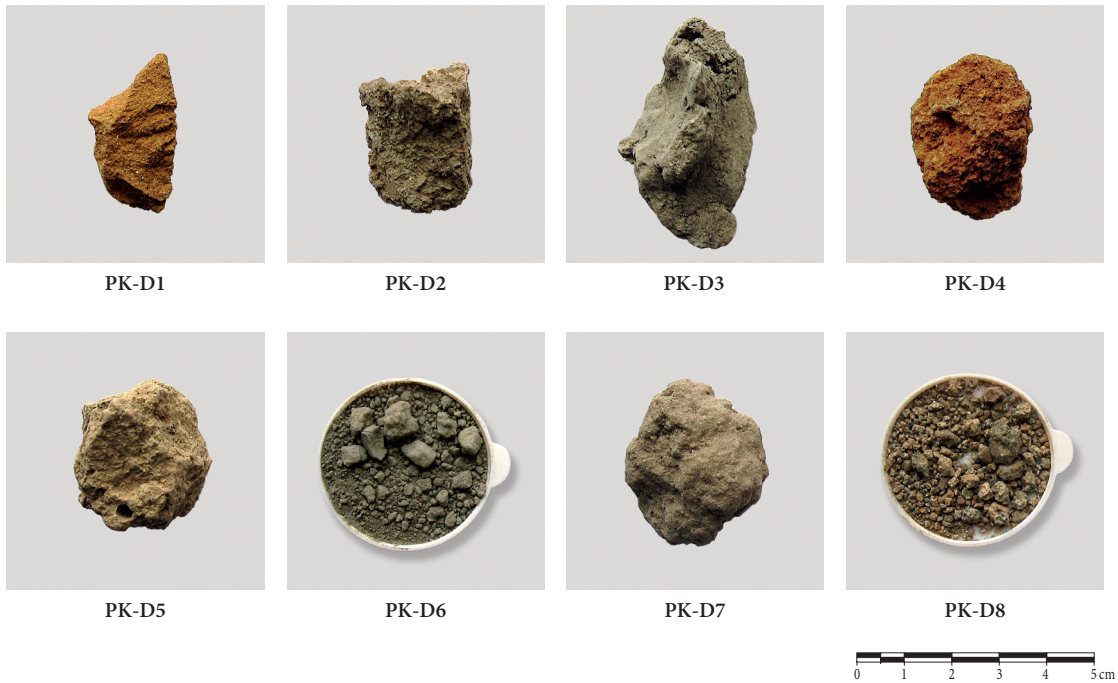


Fig. 18 Clay samples from the vicinity of Patara.

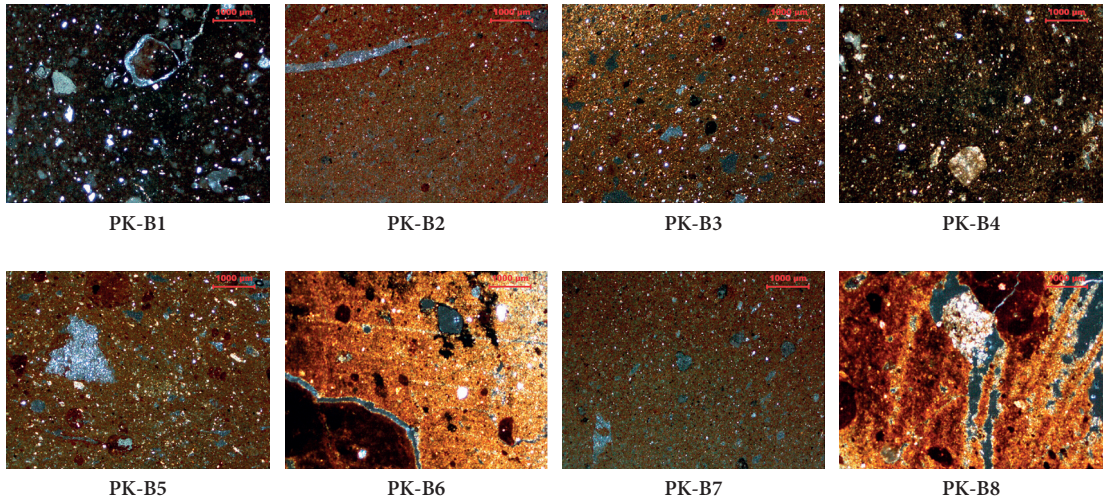


Fig. 19 Thin section microphotographs of unguentarium sherds.

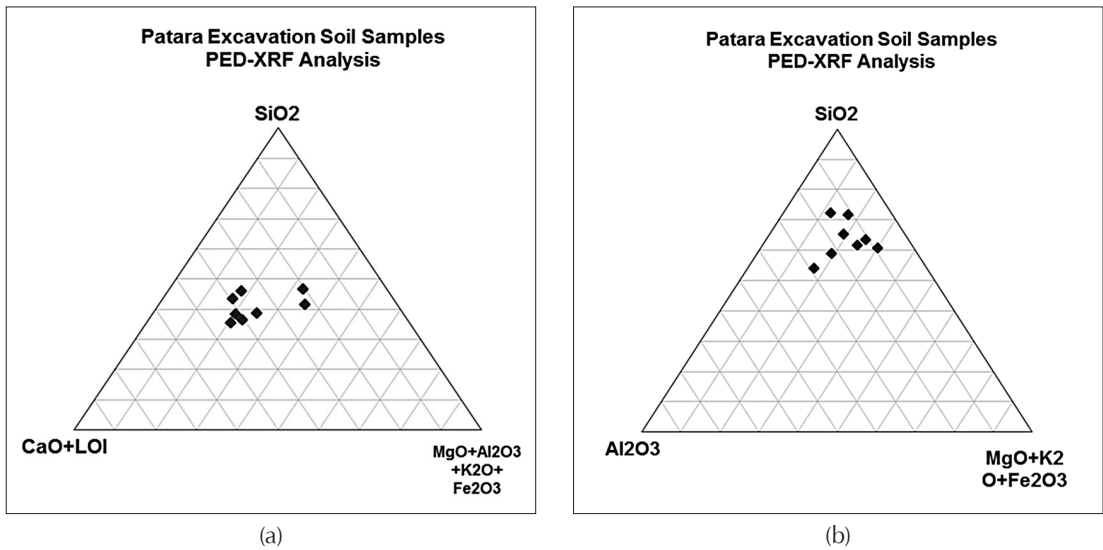


Fig. 20 a-b Grouping of soil/clay samples (Triangular Plotting):  
 (a)  $\text{SiO}_2$ - $\text{CaO}$ - $\text{LOI}$ - $\text{MgO}$ - $\text{Al}_2\text{O}_3$ - $\text{K}_2\text{O}$ - $\text{Fe}_2\text{O}_3$  ve (b)  $\text{SiO}_2$ -  $\text{Al}_2\text{O}_3$ - $\text{MgO}$ - $\text{K}_2\text{O}$ - $\text{Fe}_2\text{O}_3$

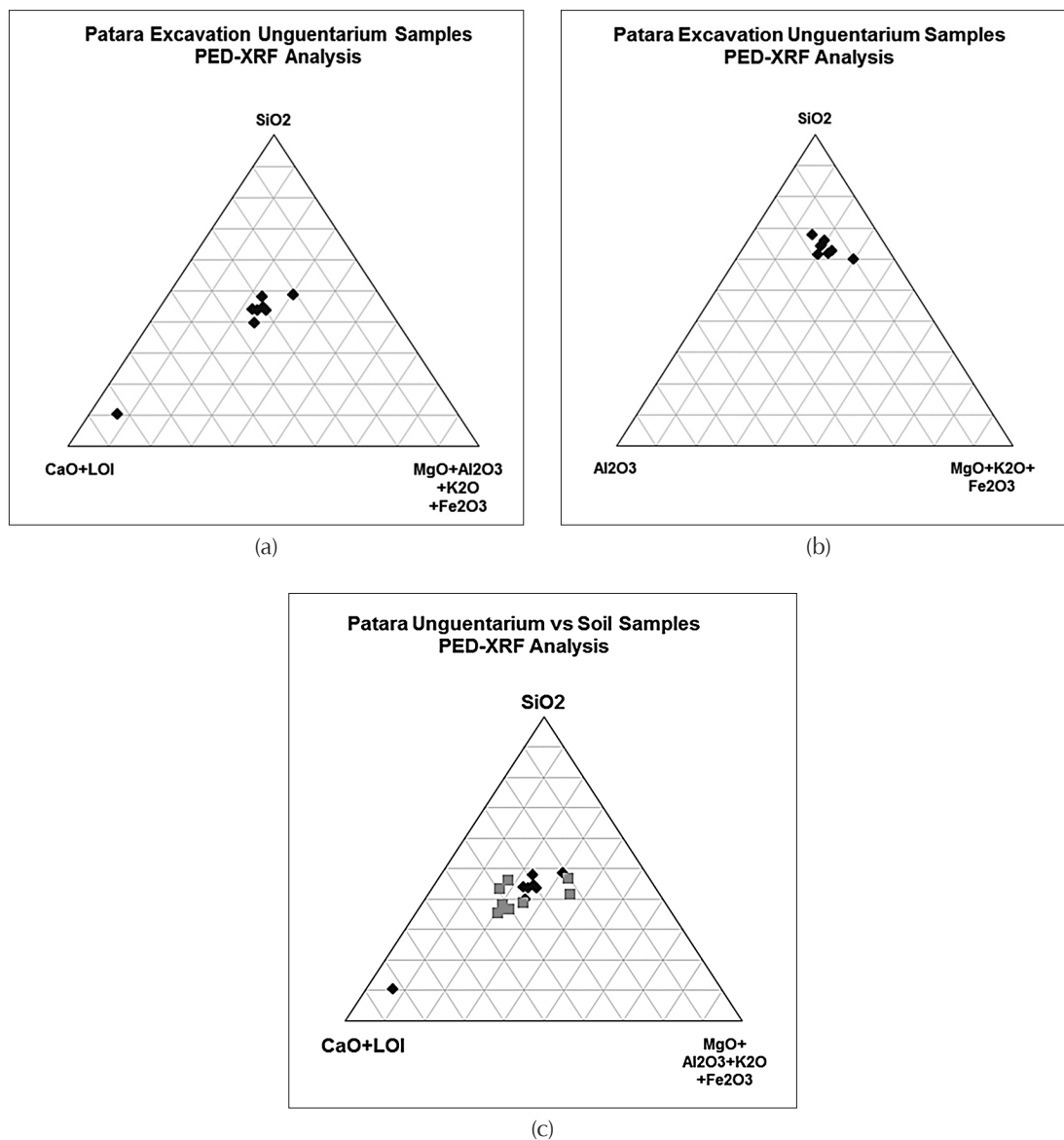


Fig. 21 a-c Unguentarium vs clay samples (Triangular Plotting):  
 (a)  $\text{SiO}_2 - \text{CaO+LOI} - \text{MgO+Al}_2\text{O}_3+\text{K}_2\text{O+Fe}_2\text{O}_3$ , (b)  $\text{SiO}_2 - \text{Al}_2\text{O}_3 - \text{MgO+K}_2\text{O+Fe}_2\text{O}_3$ ,  
 (c) unguentarium vs clays;  $\text{SiO}_2 - \text{CaO+LOI} - \text{MgO+Al}_2\text{O}_3+\text{K}_2\text{O+Fe}_2\text{O}_3$

